Determining liquid substrate cleanliness using infrared imaging

J. R. Saylor[a)]
Department of Mechanical Engineering, Clemson University, Clemson, South Carolina 29634

(Received 18 June 2001; accepted for publication 20 August 2001)

Experiments conducted in a modified Langmuir trough are described. Measurements of surface tension were obtained using a Wilhelmy plate, while infrared (IR) images of the water surface adjacent to the Wilhelmy plate were simultaneously recorded. A contaminating surfactant film was allowed to form on the surface while the experiments were being conducted. The data reveal a substantial change in the IR imagery due to the film in all cases. The difference between the appearance of the clean and surfactant-covered regions of the surface is clear and distinct. For some of these experiments the change in the IR imagery is accompanied by no observable change in surface tension. This, along with several other aspects of this work, suggest that IR imagery may be a superior tool, compared to traditional surface tension measurements, for ascertaining the cleanliness of a liquid substrate. © *2001 American Institute of Physics.*
[DOI: 10.1063/1.1416106]

I. INTRODUCTION

The study of surfactant monolayers on liquid substrates and the related subject of Langmuir–Blodgett film preparation, both require great attention to the avoidance of impurities and contaminants in the subphase, the spreading solvent, and the surfactant of interest.[1] Cleanliness is an important aspect of the study of surfactants, since extremely small quantities of impurities can result in very large differences in the quality and behavior of the surfactant monolayers subsequently formed on the liquid subphase. Many methods and laboratory practices have been developed to reduce the likelihood of contamination. However, regardless of the method chosen, some form of measurement is necessary prior to deposition to demonstrate that the substrate is indeed clean.

Ascertaining subphase cleanliness prior to surfactant deposition typically involves monitoring the surface pressure using a Wilhelmy plate as the surface is compressed to the minimum possible area of the trough being used. If there is no measurable change in surface pressure during this compression, the subphase is deemed to be sufficiently clean. Similar methods are applied to detect the presence of impurities in volatile solvents which are used as the spreading solvents for surfactants. In this case, the solvent is spread upon the liquid surface and allowed to evaporate completely. Whether any contaminants are left behind is again determined using the area reduction technique just described. The rationale in support of the use of area reduction as a means for detecting impurities is that if no measurable change in surface pressure is observed prior to surfactant deposition, then whatever impurities are actually present will result in no measurable change in surface pressure after the monolayer of interest is deposited.

Albrecht[2] demonstrated that the aforementioned method of ascertaining surface cleanliness was not valid. In a simple and incisive demonstration, Albrecht obtained pressure-area curves for a primary surfactant after purposely contaminating a water surface with a small, known quantity of a ''contaminant'' surfactant. The experiments illustrated that when a sufficiently small quantity of contaminant was deposited, no change in surface pressure could be detected using a Wilhelmy plate, even when the Langmuir trough was compressed to its minimum area. Nevertheless, when the primary surfactant was deposited, the pressure-area curve which was obtained differed substantially from that which was obtained without the introduction of a contaminant. In light of these results an alternate method for detecting contamination was suggested wherein a base-line pressure-area curve is obtained using a standard, well-characterized surfactant. Subphase cleanliness is then confirmed by comparing measured pressure-area curves for this standard surfactant with previously obtained curves.

Smaby and Brockman[3] noted that the method proposed by Albrecht[2] was limited since one is unlikely to find a standard isotherm for every combination of surfactant, subphase, temperature, *p*H, etc., which a researcher might need to investigate. As an alternative, they proposed using surface potential measurements as a means of detecting contamination, noting that surface potential is a significantly more sensitive measure of surface contamination than surface pressure.[4,5] In this method, the area of the trough is reduced, and the change in surface potential is monitored using a point probe. While this method is extremely sensitive, the authors note that the sensitivity varies from surfactant to surfactant.[6]

Herein, a method is presented wherein infrared imaging is used to detect the presence of surfactant contamination on a water surface. The ability of a surface active material to damp subsurface motion results in a change in the surface temperature field, which can be detected via infrared imaging. This method has several advantages over those described above. First and most important is that surfactant contamination is revealed in the form of a two-dimensional image. The existence *and location* of the contaminating film are readily seen, aiding perhaps in a diagnosis of the source

a)Electronic mail: jrsaylor@ces.clemson.edu

of contamination instead of simply indicating its existence. Second, no movement of the surfactant barriers is required; visualization of the subphase indicates whether the trough is ready for experimentation without having to perform a preliminary run. Moreover, because it is an imaging method, the existence of dislocated islands (perhaps far from the location of the Wilhelmy plate or surface potential measurement location) can be ascertained just as easily as for a complete contaminating monolayer. Finally, the spreading of the actual film of interest can be observed in real time, providing useful information regarding the spreading rate, degree of coverage, possible film leakage, etc. This gives real-time feedback to the researcher.

It is noted that the nonlinear optical technique, second-harmonic generation (SHG), can be used to measure the surface concentration of surfactant monolayers.[7–10] This method has typically been used as a point probe, using a single narrow laser beam. However, the availability of modern high-power lasers has permitted its application in an imaging mode by expanding the laser beam, and imaging a significant area of the interface.[11] This method provides instantaneous, nonintrusive measurements of surface concentration, and as such is a powerful tool. However, the sophisticated and expensive optics, lasers, and cameras which are necessary, currently preclude its use as a simple contamination measurement technique, like that which is described herein.

Finally, it is noted that even in the absence of contamination, differences in surfactant monolayer properties can result from different types of spreading solvents, and different methods in applying these solvents. This effect on surfactant morphology is not a contamination issue and is, therefore, not the subject of this work. The interested reader is referred to the work of Gericke, Simon-Kutscher, and Hühnerfuss,[12] which includes a review of the subject.

II. EXPERIMENTAL METHOD

The experimental facility used in these experiments is illustrated in Fig. 1. With the exception of the infrared camera, the entire experimental apparatus was located inside a laminar flow hood. The laminar flow hood contained a fan which drew room air in through a HEPA filter, providing a relatively clean, laminar air flow over the water surface. In addition to helping maintain a clean air environment in the vicinity of the water surface, the air flow served to compress the contaminant film that formed on the water surface. This compression was used as a diagnostic tool in some of the experiments described below. Except where noted, the laminar flow hood fan was kept on during all experiments.

The ''trough'' used in these experiments was not the shallow Teflon basin typical of a Langmuir facility. Rather, a custom-made glass tank, 15.2 cm×15.1 cm in area, and 9.8 cm deep was used to contain the water substrate. Surface tension of the water surface was recorded using a Wilhelmy plate composed of sand-blasted platinum, which hung from an electronic balance. Data from the balance was acquired by a PC and stored to disk. Surface tension was measured with a resolution of 0.004 dyn/cm and was acquired at a rate of 1 Hz.

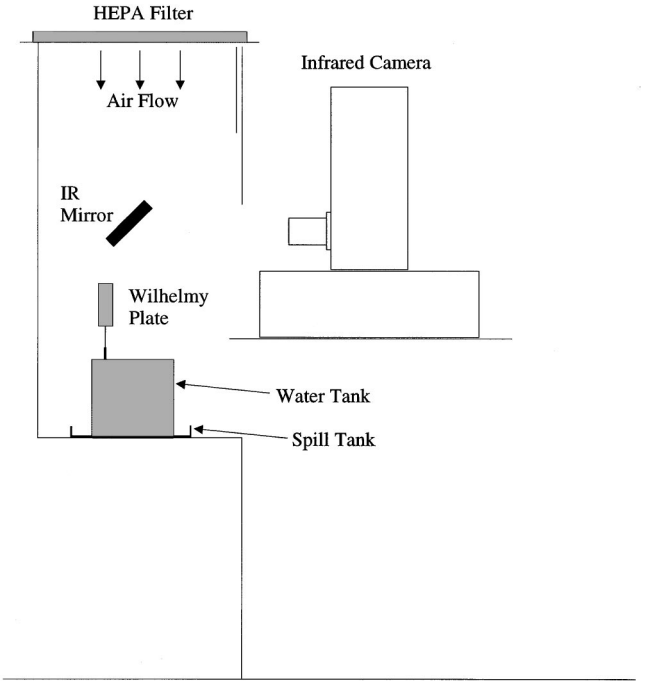

FIG. 1. Schematic illustration of the experimental setup used to obtain temperature fields from the surface of a body of water during evaporation.

As indicated in Fig. 1, the infrared camera imaged the surface of the water via a 45° bounce mirror which was located directly over the tank. The Wilhelmy plate was also located over the water surface. Its location is presented in Fig. 2 with respect to the region imaged by the infrared camera. The Wilhelmy plate is necessarily offset from the imaged region to prevent obscuration of the IR image by the Wilhelmy plate apparatus.

Infrared images of the water surface were obtained using

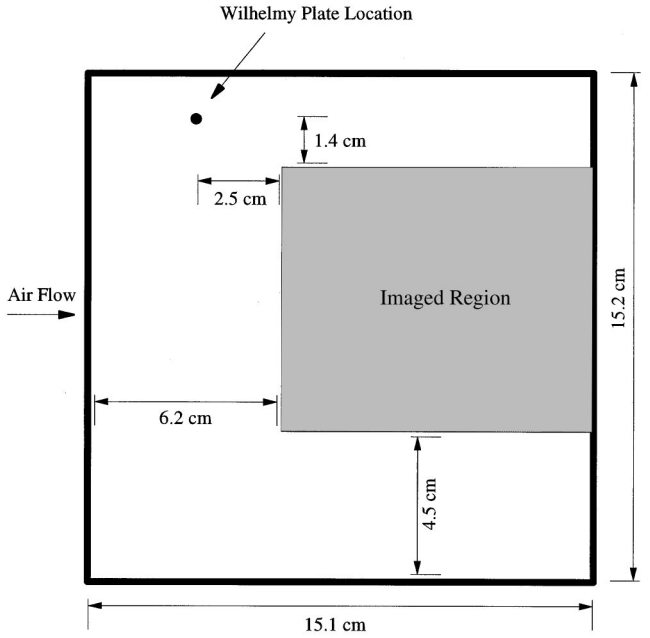

FIG. 2. Plan view of the water surface, revealing the areas imaged by the infrared camera and the Wilhelmy plate measurement location.

a Raytheon-Amber AE4256 IR camera having a 256×254 InSb array. The camera is liquid-nitrogen cooled and exhibits a noise level equivalent to approximately 25 mK in measured temperature. The region imaged was 7.9 cm×8.9 cm, as illustrated in Fig. 2. Appropriate calibrations were acquired to permit conversion of the IR imagery into surface temperature fields. In this article these calibrations were not utilized, since the conclusions drawn herein do not rely on numerical temperature values, but rather on the qualitative differences between the imagery in the clean and surfactant-covered regions.

Doubly distilled water was used as the liquid substrate in all experiments. Regardless of the type of experiment which was conducted, the following procedure was used. The distilled water was transferred to the glass tank and was sparged using dry nitrogen and a clean glass frit. This took place over an ~1 h period prior to initiation of the experiment. The tank was then briefly overflowed into a spill tank (shown in Fig. 1). The surface was then swiped with a glass rod which had been cleaned with high pressure liquid chromatography (HPLC) grade methanol and doubly distilled water, to remove any surfactant remaining in spite of the earlier cleaning steps. The Wilhelmy plate was translated vertically upward and away from the water surface during this cleaning procedure. The Wilhelmy plate was cleaned with HPLC grade methanol and doubly distilled water before each experiment. The plate was also periodically cleaned by applying a blue flame until the plate glowed orange. Upon completion of the cleaning procedure for the water surface and the Wilhelmy plate, the plate was lowered and reattached to the water surface. The water surface was then swiped one final time by sweeping the surface from a location just to the right of the Wilhelmy plate location in Fig. 2, to the right edge of the tank.

The goal of these experiments was to study the growth of a naturally occurring contaminant film. These films tend to form in spite of good cleaning procedures. In the earlier work of Saylor, Smith, and Flack,[13,14] the cleaning procedures were more rigorous than those described here, and water surfaces which were free of contaminant monolayers were attained for several tens of minutes. In the current work, the cleaning procedures were pursued with less vigor, so that the monolayer could be observed to form without unnecessarily long wait times.

To facilitate the observation of the surface temperature field, the bulk water temperature was elevated prior to initiation of the experiments. This was done to increase the heat flux from the water surface, which in turn created thermal structures which were more easily visible in the infrared imagery. The bulk water temperature was monitored throughout the experiments using a mercury in glass thermometer having a resolution of 0.1 °C. The average starting temperature for these experiments was 36 °C. During the course of the experiments, which lasted from 12 to 130 min, the water temperature decreased, resulting in an increase in the measured surface tension. This change in surface tension did not create ambiguity in the results, however, since the surfactant films investigated here grew at a much more rapid pace. As will be seen in Sec. III, the change in surface tension due to the growth of a contaminant film occurred on a time scale which was much faster than that due to the change in the bulk water temperature.

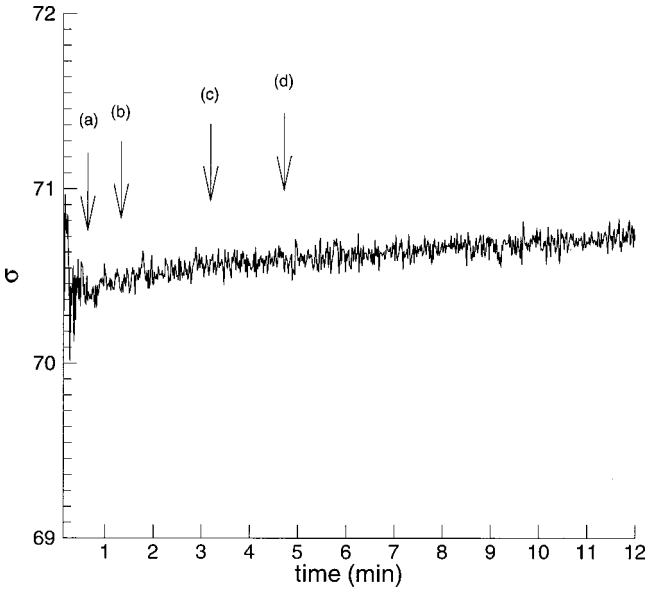

FIG. 3. Plot of surface tension (dyn/cm) as a function of time (min) for a contaminant film spreading across the water surface. Labels (a)–(d) correspond to the images presented in Fig. 4. Label (d) corresponds to the time when the film completely covers the imaged region.

In the following section the experimental results are presented. Surface tension data obtained from the Wilhelmy plate are presented in the form of surface tension versus time plots, and data from the infrared camera are presented in the form of snapshots taken from a larger sequence of images.

III. RESULTS

The experiments which were conducted are divided into three groups, each of which is described below. In each experiment, simultaneous measurements of surface tension and the surface temperature field were obtained using the Wilhelmy plate and IR camera, respectively.

A. Group 1

In the first group of experiments, a contaminant film was allowed to grow on an initially clean water surface as Wilhelmy plate and IR measurements were simultaneously acquired. Measurements were recorded from the instant of the final cleaning step, until well after the surfactant film completely covered the water surface.

A plot of surface tension versus time is presented in Fig. 3 for one of these experiments. As described in Sec. II, the tank was initially warm and cooled slightly during the course of the experiment, resulting in a slow increase in surface tension. In this experiment the tank is cooling down from an initial temperature of 33.5 °C. At the very beginning of the experiment relatively large oscillations in the data are observed. These oscillations are due to waves on the surface caused by the final swipe of the surface with a glass rod, the final step in the cleaning procedure. The noise in the overall data is higher than it otherwise would have been, due to the air flow over the water surface which disturbed the hanging Wilhelmy plate.

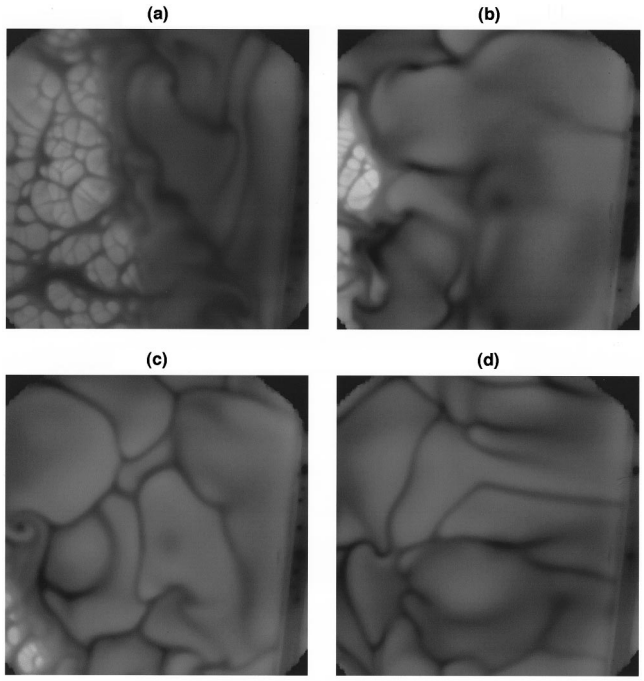

FIG. 4. Infrared images of the water surface as a contaminant film spreads from right to left. The laminar air flow is directed from left to right. Each image is a snapshot taken (a) 35 s, (b) 70 s, (c) 195 s, and (d) 295 s from the initiation of the experiment. Each snapshot corresponds to one of the labeled locations in the surface tension vs time plot presented in Fig. 3. The black pixels located in the corners of each image are regions of unresponsive pixels. The object located on the far-right edge of the image is the glass rod used to swipe the surface just prior to initiation of the experiment.

The contaminant film grew steadily across the water surface and completely covered the imaged region after about 5 min. This process is shown in Fig. 4 where snapshots of the infrared imagery data are presented at 35, 70, 195, and 295 s. The points in time when these four images were obtained are indicated by labeled arrows in the surface tension versus time plot of Fig. 3. To facilitate further discussion of the IR images presented herein, an explanation of the general nature of structures observed in infrared imagery during evaporative convection is now presented.

When a water surface is exposed to air having a relative humidity less than 100%, evaporation occurs, thereby cooling the surface. The cooling of the surface renders it unstable, and surface water falls downward and is replaced by warmer bulk water. This process is referred to as evaporative convection.[15] Several researchers have noted that the large-scale flow observed in evaporative convection consists of thin, falling sheets having a relatively large velocity, interspersed with larger rising plumes having a smaller velocity.[15–19] These falling sheets are observed as dark or black lines in infrared imagery, and the plumes as broad white or light gray areas. Such dark lines and light gray plumes are observed throughout the imagery in Fig. 4.

When any surfactant film having a finite elasticity is present, motion at or near the water surface is damped. Figure 5 shows a pair of infrared images due to Saylor, Smith, and Flack.[13] These two images were obtained under identical conditions, the only difference being that a surfactant monolayer is present on the water surface for the image on the

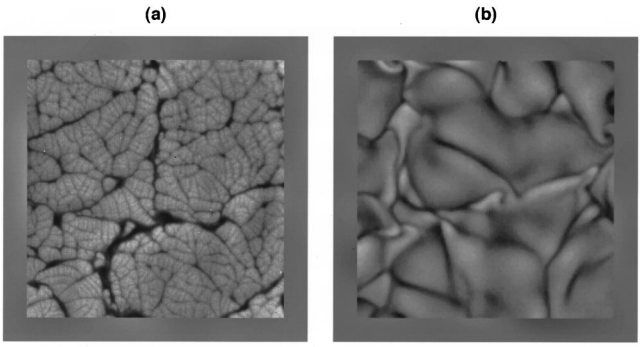

FIG. 5. Infrared images of (a) a clean water surface and (b) a surface covered with a monolayer of oleyl alcohol. The heat fluxes are the same in (a) and (b).

right. The evaporation rates and heat fluxes for the two images are the same, because the surfactant monolayer is oleyl alcohol, which does not inhibit evaporation.[20] As a result, the difference in these two images is solely due to the ability of a surfactant monolayer to damp subsurface motion. These images clearly show the dramatic difference in the spatial structures of the surface temperature field caused by the presence of a surfactant. The clean surface shows a broad range of spatial scales, from very small to very large, while the image of the surfactant-coated surface shows only large-scale structures present. This is the hallmark of the effect of a surfactant film on the temperature field, and has been observed in other studies.[14,21,22]

Referring back to Fig. 4, the same difference between clean-surface and surfactant-covered-surface behavior observed in Fig. 5 is also observed in Fig. 4(a), where two distinct regions are seen. On the right-hand side of Fig. 4(a), there is a well-defined dark region where only large-scale structures exist, separated from a bright region on the left-hand side of the image where a broad range of spatial scale structures can be seen. The boundary between this dark and bright region in Fig. 4(a) is indicative of a spreading surfactant film front.[21] This front is spreading across the surface from right to left in the image sequence, Figs. 4(a)–4(d). The air flow, which travels from left to right, is the force which keeps the film confined to the right side of the tank as it grows. This last point is confirmed by the group 3 experiments presented below.

The points in time where each of the IR images of Fig. 4 were acquired are indicated by labeled arrows in Fig. 3. The Wilhelmy plate is not visible in the images presented in Fig. 4 and is located just outside of the upper-left-hand corner of the IR images, as shown in Fig. 2. Hence, shortly after the time corresponding to point (d) in Fig. 3 this film crosses the Wilhelmy plate measurement location. It is important to note that at no time in Fig. 3 is there an easily discernible, sudden drop in surface tension which would be expected when the film crosses the location of the Wilhelmy plate. No such drop is observed in the vicinity of point (d) in Fig. 3, or at any time in the more than 7 min after point (d). This might suggest that the contaminant film has no surface-tension-lowering properties. This is unlikely, however, since the contaminant film is sufficiently surface active to damp out the

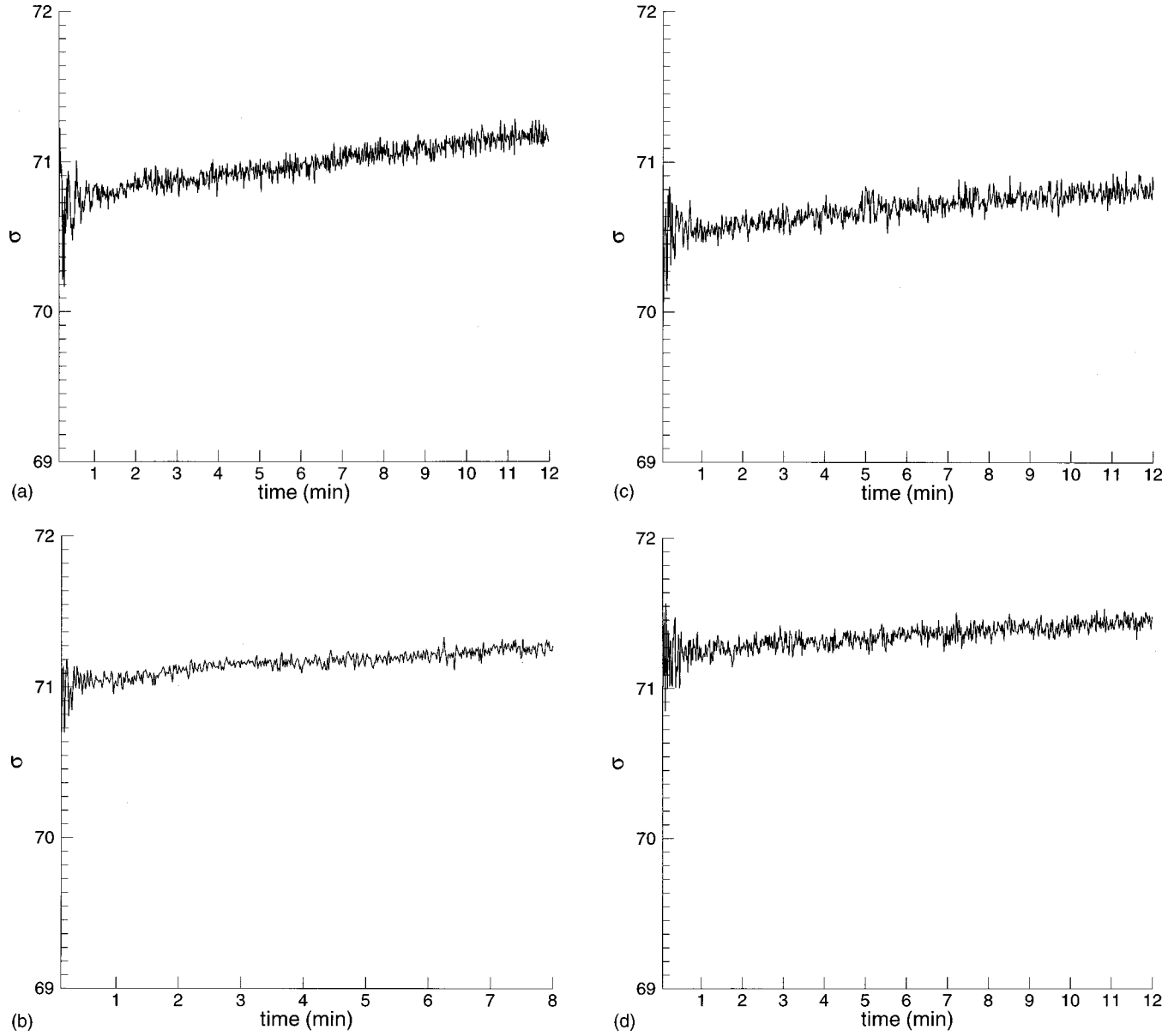

FIG. 6. (a)–(d) Plot of surface tension (dyn/cm) as a function of time (min) for four different contaminant films spreading across a water surface.

subsurface fluid flow structures which are eminently visible in the IR imagery of Fig. 4. This point will be revisited in Sec. IV.

Four more experiments of this type were conducted in addition to the one plotted in Fig. 3. Each of these experiments was conducted under conditions essentially identical to those of Fig. 3. The surface tension data and infrared images obtained in these experiments are similar to those presented above. The surface tension versus time plots for these experiments are presented in Fig. 6 for the sake of completeness.

B. Group 2

It could be argued that the behavior observed in Fig. 4 is due to something other than a surfactant film, an argument which could be supported by the lack of a measurable change in surface tension. This possibility is addressed in the following group of experiments where a contaminant film was allowed to grow and was subsequently compressed, while checking for changes in surface tension.

A plot of surface tension versus time is presented in Fig. 7 during which the contaminant film was compressed. Compression was achieved by pushing a glass rod across the tank, beginning at the tank edge and ending at the edge of the imaged region. This resulted in a compression from the initial total tank area of 229.5 cm^2 to an area of 88.1 cm^2. The change in σ due to this factor of 2.6 compression is revealed in Fig. 7. The beginning and end of the compression are marked by large oscillations in σ caused by the glass rod, which created small capillary waves at the initiation and cessation of its motion. The compression resulted in a $\sim$0.2 dyn/cm reduction in σ, proving that there is indeed a surfactant film on the water surface. In Fig. 8, the film is compressed by a factor of 1.3, half that for Fig. 7. As can be seen in Fig. 8, the decrease in surface tension is smaller, on the order of $\sim$0.1 dyn/cm.

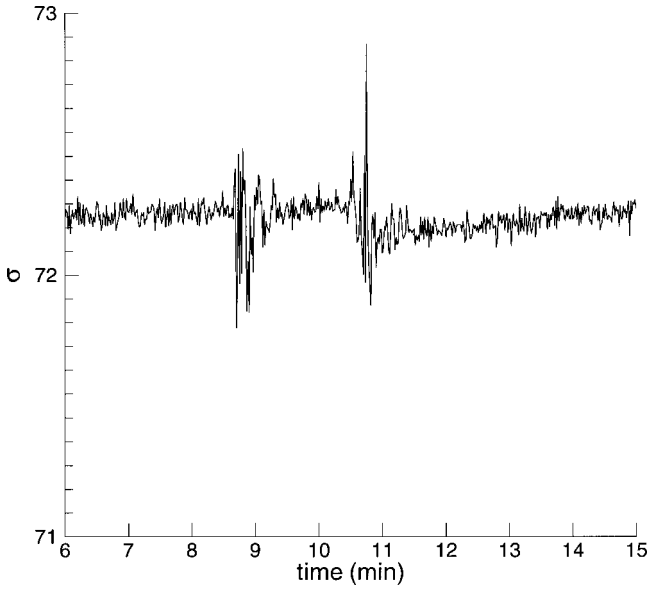

FIG. 7. Plot of surface tension (dyn/cm) as a function of time (min) for a contaminant film. The film is compressed by a factor of 2.6. The compression occurs between the regions where the signal is seen to exhibit large oscillations. At the beginning of the film compression, the film had already grown to cover the entire imaged region.

The measured change in surface tension due to compression must be due to the presence of a surfactant film. However, the data presented in Figs. 7 and 8 do not necessarily prove that this film is the same as what *appears* to be a film in the infrared imagery. This is demonstrated in Fig. 9, where an IR image is presented shortly after the contaminant film is compressed by a factor of 1.3. At this compression, the glass rod used to compress the film is located within the imaged region. To the left of the rod is the region being compressed as well as the location of the Wilhelmy plate, which gives a reduced measurement during compression. The fact that the region to the left of the rod appears almost identical to that of

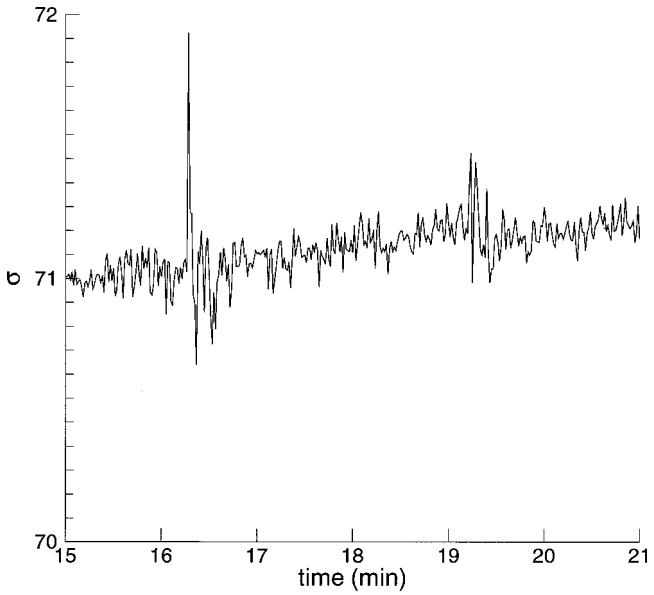

FIG. 8. Plot of surface tension (dyn/cm) as a function of time (min) for a contaminant film. The film is compressed by a factor exactly half that of Fig. 7, e.g., 1.3. All other conditions are the same as for Fig. 7.

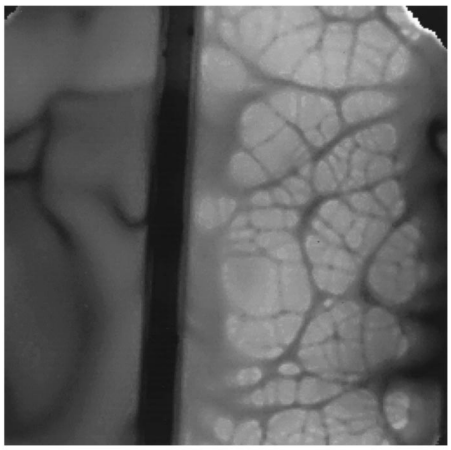

FIG. 9. Infrared image of the water surface just after a contaminant film undergoes a factor of 1.3 compression. Ahead of the glass rod, the IR behavior is that of a surfactant-covered surface, while the region behind the rod displays behavior characteristic of a clean water surface.

Fig. 5(b), i.e., surfactant behavior, while the region to the right of the rod displays the clean behavior seen in Fig. 5(a), strongly suggests that what appears to be a surfactant film in the IR imagery is indeed just that.

C. Group 3

In the final group of experiments, a contaminant film was allowed to grow until it covered half of the imaged area. At this point, the laminar air flow was turned off, eliminating the force keeping the film in place. A sequence of infrared images is presented in Fig. 10, which show the surfactant film quickly expanding across the water surface when the air

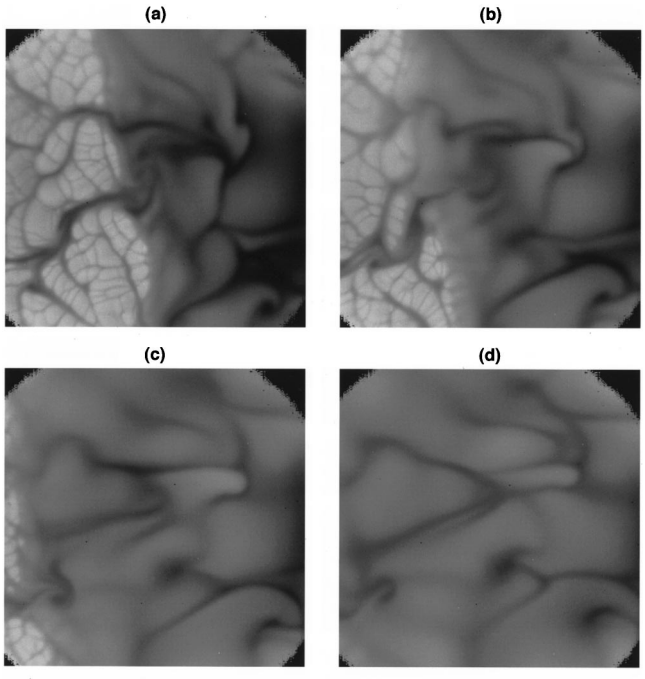

FIG. 10. Sequence of infrared images showing the sudden expansion of a contaminant film as the air flow is turned off. The times after experiment initiation at which the images were obtained are (a) 280 s, (b) 284 s, (c) 288 s, and (d) 292 s.

flow ceases. Note that these images are separated in time by only 4 s. This is further evidence for the presence of a surfactant film; some type of elasticity would be necessary for this type of expanding behavior to be observed.

IV. DISCUSSION

The data provided by the group 1 experiments show no sudden change in measured surface tension as a dark region which appears to be a surfactant film moves across the water surface in the infrared images. A slow, gradual increase in surface tension is observed. This gradual increase does not seem to be explained by a surfactant effect, since the encroaching surfactant film in Figs. 4(a)–4(d) exhibits a very sharply defined boundary. The change in surface tension is, therefore, most likely due to the gradually decreasing water temperature.

The data presented in the group 2 experiments provide stronger evidence for the conclusion that the dark region observed in the infrared imagery is a surfactant film. Here, compression of the surface results in a measurable reduction in σ, as such a compression of a surfactant film should. Furthermore, as the film is being compressed, the region behind the glass rod redisplays the clean behavior which had been observed ahead of the encroaching film in Fig. 4 and is very similar to the clean infrared image in Fig. 5(a).

A characteristic of surfactant films is their elasticity: resistance to compression and reexpansion when released. This characteristic is seen in the group 3 data, where the film can be seen to expand across the surface as the air flow, which had been compressing it, is turned off.

Taken as a whole, the above results suggest that the dark area which has relatively large-scale thermal structures, seen in the IR imagery of Figs. 4 and 10, is a surfactant film. It is noted that this film is easily visible, contrasting strongly with the clean portion of the surface. And, this easily visible film is one which has a very small (immeasurably small in some cases) effect on σ. Consequently, it is suggested that this method would serve quite well in detecting surface contaminants. It is especially well suited because the cause of the change in the surface imagery is the elasticity of the film, which damps subsurface motion. Hence, contaminants which most affect σ will be most visible.

It is noted that the method described here requires some type of subsurface flow in order to function. Otherwise, there is no flow to damp and, therefore, no visual contrast between the clean and contaminated regions. Typically, this flow is evaporation-driven natural convection (evaporative convection) in the trough. Such evaporative convection should be observed in many facilities, where relatively low-humidity laboratory air is drawn into a laminar flow hood. However, in situations where the researcher purposely seeks to attain 100% relative humidity above the trough in order to eliminate temperature variations caused by evaporation, the method described here will fail. A possible procedure which can be utilized in such a situation would be to impose a low-humidity air flow first, to ascertain surface cleanliness, and then cover the trough so that the humidity would rise, and proceed with the experiment. This method should be even more effective when the subphase is a volatile liquid.

ACKNOWLEDGMENTS

Financial support from the Office of Naval Research through the Naval Research Laboratory is gratefully acknowledged.

[1] G. L. J. Gaines, *Insoluble Monolayers at Liquid–Gas Interfaces* (Wiley, New York, 1966).
[2] O. Albrecht, Thin Solid Films **178**, 563 (1989).
[3] J. M. Smaby and H. L. Brockman, Chem. Phys. Lipids **58**, 249 (1991).
[4] D. A. Cadenhead and B. M. J. Kellner, J. Colloid Interface Sci. **49**, 143 (1974).
[5] H. Morgan, D. M. Taylor, and O. N. Oliveira, Thin Solid Films **178**, 73 (1989).
[6] J. M. Smaby and H. L. Brockman, Biophys. J. **58**, 195 (1990).
[7] Y. R. Shen, Nature (London) **337**, 519 (1989).
[8] M. J. Vogel, A. H. Hirsa, J. S. Kelley, and G. M. Korenowski, Rev. Sci. Instrum. **72**, 1502 (2001).
[9] A. Hirsa, G. M. Korenowski, L. M. Logory, and C. D. Judd, Exp. Fluids **22**, 239 (1997).
[10] A. Hirsa, G. M. Korenowski, L. M. Logory, and C. D. Judd, Langmuir **13**, 3813 (1997).
[11] G. M. Korenowski, J. R. Saylor, A. J. Szeri, and E. A. Van Wagenen, in *52nd Annual Meeting of the Division of Fluid Dynamics of the American Physical Society* (AIP, New York, 1999).
[12] A. Gericke, J. Simon-Kutscher, and H. Hühnerfuss, Langmuir **9**, 2119 (1993).
[13] J. R. Saylor, G. B. Smith, and K. A. Flack, Int. J. Heat Mass Transf. **43**, 3073 (2000).
[14] J. R. Saylor, G. B. Smith, and K. A. Flack, Phys. Fluids **13**, 428 (2001).
[15] J. C. Berg, A. Acrivos, and M. Boudart, in *Advances in Chemical Engineering*, edited by T. B. Drew, J. W. Hoopes, T. Vermeulen, and C. G. R. (Academic, New York, 1966), pp. 61–124.
[16] W. G. Spangenberg and W. R. Rowland, Phys. Fluids **4**, 743 (1961).
[17] T. D. Foster, Phys. Fluids **8**, 1770 (1965).
[18] K. B. Katsaros, W. T. Liu, J. A. Businger, and J. E. Tillman, J. Fluid Mech. **83**, 311 (1977).
[19] R. J. Volino and G. B. Smith, Exp. Fluids **27**, 70 (1999).
[20] K. B. Katsaros and W. D. Garrett, Int. J. Heat Mass Transf. **25**, 1661 (1982).
[21] J. R. Saylor, G. B. Smith, and K. A. Flack, Phys. Fluids **12**, 597 (2000).
[22] J. R. Saylor, K. A. Flack, M. P. Schultz, and G. B. Smith, Exp. Fluids (to be published).